SUPPORTING INFORMATION

Weighting and indirect effects identify keystone species in food webs

Lei Zhao[a, b], Huayong Zhang[* a], Eoin J. O'Gorman[b], Wang Tian[a], Athen Ma[c],

John C. Moore[d, e], Stuart R. Borrett[f, g], and Guy Woodward[b]

[a] *Research Center for Engineering Ecology and Nonlinear Science, North China Electric Power University, Beijing, 102206, China*

[b] *Department of Life Sciences, Imperial College London, Silwood Park Campus, Buckhurst Road, Ascot, Berkshire, SL5 7PY, UK*

[c] *School of Electronic Engineering and Computer Science, Queen Mary, University of London, Mile End Road, London, E1 4NS, UK*

[d] *Department of Ecosystem Science and Sustainability, Colorado State University, Fort Collins, CO 80523, USA*

[e] *Natural Resource Ecology Laboratory, Colorado State University, Fort Collins, CO 80523, USA*

[f] *Department of Biology and Marine Biology, University of North Carolina Wilmington,, Wilmington, NC 28403, USA*

[g] *Duke Network Analysis Center, Duke University, Durham, NC 27708, USA*

*Corresponding author: Huayong Zhang, E-mail: rceens@ncepu.edu.cn

Supplementary Methods and Analyses

Appendix S1. Calculating weighted directed connectance.

Appendix S2. "Green" webs and "brown" webs.

Appendix S3. Effects of food web shrinkage during the node deletion process.

Supplementary Tables

Table S1. Multiple comparisons of robustness (R_{50}) or survival area (SA) under four different deletion sequences, with different functional responses.

Table S2. Taxa with the three highest values for the four deletion orders in each food web.

Supplemental Figures

Figure S1. Scheme of dynamical model construction based on carbon flux.

Figure S2. Stability, represented by (a) robustness, R_{50}, and (b) survival area, SA, to species loss in four deletion sequences with a linear functional response.

Figure S3. Stability, represented by (a) robustness, R_{50}, and (b) survival area, SA, to species loss in four deletion sequences in five groups of hill exponent, h, with a nonlinear functional response.

Figure S4. Stability, represented by (a) robustness, R_{50}, and (b) survival area, SA, to species loss in four deletion sequences in five groups of carrying capacity coefficient, k_0, with a nonlinear functional response.

Figure S5. Stability, represented by (a) robustness, R_{50}, and (b) survival area, SA, to species loss in four deletion sequences in five groups of half-saturation coefficient, b, with a nonlinear functional response.

Figure S6. Stability, represented by (a) robustness, R_{50}, and (b) survival area, *SA*, to species loss in four deletion sequences in five groups of predator interference coefficient, *q*, with a nonlinear functional response.

Figure S7. Stability, represented by (a) robustness, R_{50}, and (b) survival area, *SA*, to species loss in four deletion sequences in five groups of carrying capacity coefficient, k_0, with a linear functional response.

Figure S8. Stability in linear functional response simulations indicated by robustness, R_{50}, and survival area, *SA*, as a function of the taxon richness *S* and weighted connectance, C_w of each web.

Figure S9. Linear regression of average logarithmic biomass and taxon richness of 20 food webs.

Figure S10. Comparison of energy channels from producers and detritus.

Figure S11. The ratios of detritus storage (DS) to daily net primary production (NPP) and daily respiration of the detritus-based food web (R).

Figure S12. Stability, represented by survival area (*SA*), to species loss in four deletion sequences, when the criterion to end the simulation once all producers were extinct was applied.

Figure S13. The ratio of the fractions of taxa that have to be removed to cause a food web to lose 0-50% (R_1) and 50-100% (R_2) of its living taxa for the four deletion sequences.

Figure S14. The proportion of relative food web sizes (the ratio of the size after deletion to the starting size) in ten size classes for the four deletion sequences.

Figure S15. Pielou's evenness of the distribution of relative food web sizes in ten size classes for the four deletion sequences and uniform distribution.

Supplementary References

Appendix S1. Calculating weighted directed connectance

Here we summarized the method for calculating weighted directed connectance C_w after Banašek-Richter *et al.*(2009): a food web with S species can be represented by an S-by-S quantitative food-web matrix $\boldsymbol{b} = [b_{ij}]$; the value of the element b_{ij} means the amount of biomass passing from taxon i to taxon j per unit area and time; for taxon k, we can measure the diversity of the biomass coming from its resources ($H_{R,k}$) and of that going to its consumers ($H_{C,k}$), i.e. the taxon-specific Shannon indices of inflows and outflows:

$$H_{R,k} = -\sum_{i=1}^{S} \frac{b_{ik}}{b_{\square k}} \ln \frac{b_{ik}}{b_{\square k}} \quad (1)$$

$$H_{C,k} = -\sum_{j=1}^{S} \frac{b_{kj}}{b_{k\square}} \ln \frac{b_{kj}}{b_{k\square}} \quad (2)$$

Here $b_{\square k}$ means the sum of column k, while $b_{k\square}$ represents the sum of row k. The effective number of resources ($N_{R,k}$) and consumers ($N_{C,k}$) are:

$$N_{R,k} = \exp(H_{R,k}) \quad (3)$$

$$N_{C,k} = \exp(H_{C,k}) \quad (4)$$

The weighted link density (LD_w) is:

$$LD_w = \frac{1}{2b_{\square\square}} \left(\sum_{k=1}^{S} b_{\square k} N_{R,k} + \sum_{k=1}^{S} b_{k\square} N_{C,k} \right) \quad (5)$$

where $b_{\square\square}$ is the total sum of the matrix. Lastly, the weighted directed connectance (C_w) can be obtained as following:

$$C_w = \frac{LD_w}{S} \quad (6)$$

Appendix S2. "Green" webs and "brown" webs

During the sequential deletions, it was possible for all producers to go extinct. One logical way to deal with this issue may be to discard any simulations where this occurred, to avoid including food webs with no autotrophic energy in the analyses. However, since food webs can be divided into producer-based ("green") and detritus-based ("brown") sub-webs (Butler *et al.* 2008; Rooney *et al.* 2008), the brown food webs may still function and persist for a long time if the detrital taxa have sufficient carbon storage. In the main text, we let the dynamical model determine the loss of nodes based on the energy budget, rather than making the judgment artificially (based on presence and absence of both green and brown sub-webs). In this section, we explore the relative sizes of the two sub webs and the detritus storage for each ecosystem. Furthermore, we tested whether our conclusions are altered if we add the new criterion that simulations are discarded when all producers go extinct.

First, we explored the role of detritus in the 20 food webs. A method proposed by Rooney *et al.* (2008) was used to calculate the proportion of carbon derived from producers and detritus:

$$\%BR_C = \sum_{1}^{n} P_C \times \%BR_R \qquad (7)$$

where $\%BR_C$ means the proportion of carbon derived from basal resources, n is the number of resources consumed by the consumer, P_C is the proportion of the consumer diet accounted for by a resource, and $\%BR_R$ means the proportion of carbon derived from the basal resource in the resource being consumed. Using this method, we calculated the proportion of "green" energy and "brown" energy for each node in each food web (see Fig. S10a for an example). If a node obtained more than half of its energy from producers, we counted it in the green sub-web; if it derived more energy from detritus, we counted it in the brown sub-web. We found that, on average, 43% of

nodes were detritus-based, and 30% of the 20 food webs were dominated by brown webs (see Fig. S10b).

The average carbon storage of detritus in the 20 ecosystems was approximately equal to the accumulated net primary production after 186 days (Fig. S11). The average carbon storage of detritus supported 603 days of brown web respiration, assuming that all the taxa in the brown webs had constant respiration. In reality, the population biomass and respiration of consumers would decrease as energy from producers is cut off. The exhaustion of detritus would also decrease the total biomass and thus the total energy demand of the brown webs, which would extend the persistent period of brown webs even further.

Considering the large size of detritus-based food webs and the large storage of detritus, it would be reasonable to let the dynamical model determine the loss of nodes based on the energy budget. However, it is still useful to explore whether our conclusions are altered if we add the criterion that the simulations are discarded if all producers go extinct. In this case R_{50}, the fraction of taxa that have to be removed in order to induce $\geqslant$50% total taxon loss, may not be reached in some food webs because all producers go extinct earlier than half of the total taxa. Thus we only used survival area, *SA*, to test if our conclusions held. Based on our results, the three new indices led to significantly lower stability than Max.D (see Fig. S12, $z = -2.831$, $P = 0.028$ for Max.DI; $z = -6.098$, $P < 0.001$ for Max.wD; $z = -3.771$, $P = 0.001$ for Max.wDI), so our major conclusion was not altered.

Appendix S3 Effects of food web shrinkage during the node deletion process

During the sequential deletion process, the size of the food webs kept decreasing as primary and secondary extinctions occurred. In this section, we test whether this web shrinkage would affect the comparison among deletion sequences. This question can be separated into two parts: (1) whether stability changed as the food webs shrank in size during species deletion; and (2) whether large and small webs were equally represented in the four deletion sequences.

First, we tested if stability changed as the food webs shrank in size during node deletion. Let R_1 and R_2 be the fractions of taxa that have to be removed to cause a food web to lose 0-50% and 50-100% of its living taxa, respectively. If stability increases as food webs shrink, we would expect $R_1/R_2 < 1$, i.e. fewer primary deletions are needed to lose the first 50% of living taxa compared to the last 50%. We found that this ratio was not significantly different from 1 for the deletion orders Max.D (*t*-test: $t_{19} = -0.568$, $P = 0.577$) and Max.wDI ($t_{19} = -1.066$, $P = 0.300$), but it was significantly less than 1 for Max.DI ($t_{19} = -2.505$, $P = 0.011$) and Max.wD ($t_{19} = -3.246$, $P = 0.002$). The average values of R_1/R_2 were all close to 1, however (see Fig. S13; 0.973 ± 0.048 (mean ± SEM), 0.787 ± 0.085, 0.800 ± 0.062, and 0.912 ± 0.083 for Max.D, Max.DI, Max.wD, and Max.wDI, respectively), indicating that stability did not change much as food webs shrank during species deletion.

Second, we tested if small and large webs were equally represented for each deletion sequence. We binned the relative size of the food webs (the ratio of the size after deletion to the starting size) into ten size classes and calculated the proportion for each size class (see Fig. S14). We then calculated the Pielou's evenness of the relative size distribution for each deletion sequence for each web. To test if the relative size was evenly distributed, for each web we conducted 1,000 Monte Carlo

simulations. In each simulation, *N* random numbers from U[0, 1] were generated. *N* is the mean number of deletions for the four deletion sequences, representing the number of web sizes in deletion sequences. The proportions of these numbers in the ten bins were counted and Pielou's evenness was calculated for each simulation for each web. The mean evenness of the 1,000 simulations was used to compare with the evenness of the four deletion sequences, using a linear mixed effects model (LME) with a maximum-likelihood estimator (function 'lme' with 'method = ML' within the 'nlme' package in R 3.2.3). Food web identity was included in the model as a random factor. Post-hoc comparisons were applied using the Tukey HSD test at $\alpha = 0.05$ level of significance (function 'glht' within the 'multcomp' package).

The evenness of Max.D ($z = -4.960$, $P < 0.001$) and Max.DI ($z = --3.661$, $P = 0.003$) were significantly less even than the uniform distribution, while Max.wD ($z = -1.185$, $P = 1$) and Max.wDI ($z = -1.859$, $P = 0.631$) were not significantly different from the uniform distribution (Fig. S15). Among the four deletion sequences, only two pairs showed significant differences in evenness ($z = 3.775$, $P = 0.002$ for Max.D *vs* Max.wD; $z = 3.102$, $P = 0.019$ for Max.D *vs* Max.wDI). The average evenness of the four deletion sequences (0.228 ± 0.014, 0.239 ± 0.010, 0.260 ± 0.013, and 0.254 ± 0.014 respectively) were very close to the uniform distributions (0.270 ± 0.013), suggesting that food web sizes were evenly distributed and there was negligible bias towards small or large webs.

Table S1. Multiple comparisons of robustness (R_{50}) or survival area (SA) under four different deletion sequences, with different functional responses. Significant results ($P < 0.05$) are shown in bold.

Functional response	Stability	Deletion sequences	Max.D	Max.DI	Max.wD	Max.wDI
Nonlinear	R_{50}	Max.D	—	**-4.469**	**-5.836**	**-4.575**
		Max.DI		—	-1.367	-0.106
		Max.wD			—	1.261
		Max.wDI				—
	SA	Max.D	—	**-3.823**	**-5.631**	**-4.602**
		Max.DI		—	-1.808	-0.779
		Max.wD			—	1.029
		Max.wDI				—
Linear	R_{50}	Max.D	—	**-3.247**	**-5.728**	**-4.733**
		Max.DI		—	-2.481	-1.487
		Max.wD			—	0.995
		Max.wDI				—
	SA	Max.D	—	**-4.856**	**-8.274**	**-6.377**
		Max.DI		—	**-3.417**	-1.521
		Max.wD			—	1.896
		Max.wDI				—

Table S2. Taxa with the three highest values for the four deletion orders in each food web.

Food web	Max.D	Max.DI	Max.wD	Max.wDI
Bothnian Bay	Mesozooplakton	Macrofauna	Bacteria	Meiofauna
	Dem. Fish	Meiofauna	Microzooplakton	Bacteria
	Macrofauna	Mesozooplakton	Mesozooplakton	Microzooplakton
Baltic Sea	Deposit Feeders	Deposit Feeders	Mesozooplakton	Mesozooplakton
	Benthis Invertebrate Carnivores	Meiofauna	Pelagic Production	Deposit Feeders
	Mesozooplakton	Mesozooplakton	Microzooplankton	Pelagic Production
Ems Estuary	Benthis Invertebrate Carnivores	Benthis Invertebrate Carnivores	Meiofauna	Microzooplankton
	Microzooplankton	Meiofauna	Microzooplankton	Meiofauna
	Mesozooplankton	Microzooplankton	Benthis Producers	Pelagic Producers
Swartkops	Planktivorous Fish	Microzooplankton	Benthic Suspention Feeders	Benthic Suspention Feeders
	Microzooplankton	Planktivorous Fish	Benthis Producers	Benthis Producers
	Mesozooplankton	Mesozooplankton	Meiofauna	Microzooplankton
Crystal River	Benthis Invertebrate Carnivores	Benthis Invertebrate Carnivores	Macrophytes	Benthis Invertebrate Carnivores
	Gulf Killifish	Zooplankton	Benthis Invertebrate Carnivores	Macrophytes
	Pinfish	Pinfish	Microphytes	Microphytes
Benguela	Hake	Microplankton	Bacteria	Microplankton
	Carnivorous Fish	Phytoplankton	Phytoplankton	Bacteria
	Macrozooplankton	Mesozooplankton	Mesozooplankton	Phytoplankton

Neuse Estuary	Meiobenthos	Meiobenthos	Free living bacteria	Sediment bacteria
	Demersal fish	Sediment bacteria	Sediment bacteria	Zooplankton
	Pelagic-demersal fish	Dep. feed. polychaetes	Zooplankton	Free living bacteria
Georges Bank	Macrobenthos- crustace	Macrobenthos- other	Phytoplankton- Primary	Phytoplankton- Primary
	Macrobenthos- other	Macrobenthos- crustace	Small copepods	Macrobenthos- other
	Demersals- piscivores	Sharks- pelagics	Bacteria	Bacteria
Gulf of Maine	Macrobenthos- crustacea	Macrobenthos- crustacea	Large Copepods	Large Copepods
	Macrobenthos- other	Macrobenthos- other	Phytoplankton- Primary	Phytoplankton- Primary
	Demersals- omnivores	Demersals- omnivores	Small copepods	Bacteria
Narragansett	Ben Macrofauna	Mesozooplankton	SedPOC Bacteria	SedPOC Bacteria
	Shrimp(Pal+Crg)	Phytoplankton	Pelag Bacteria	Pelag Bacteria
	Mesozooplankton	Shrimp(Pal+Crg)	Mesozooplankton	Phytoplankton
Atlantic Bight	Macrobenthos- crustace	Macrobenthos- crustace	Bacteria	Macrobenthos- other
	Macrobenthos- other	Macrobenthos- other	Phytoplankton- Primary	Bacteria
	Small Pelagics- commer	Sharks- coastal	Macrobenthos- other	Phytoplankton- Primary
New England	Macrobenthos- crustace	Macrobenthos- crustace	Phytoplankton- Primary	Phytoplankton- Primary
	Macrobenthos- other	Macrobenthos- other	Bacteria	Bacteria
	Demersals- omnivores	Sharks- pelagics	Small copepods	Small copepods
Chesapeake	Zooplankton	Bacteria in sediment POC	Bacteria in sediment POC	Bacteria in sediment POC
	Bacteria in suspended POC	Blue Crab	Phytoplankton	Phytoplankton
	Bay Anchovy	Zooplankton	Free Bacteria	Other Polychaetes
St. Marks	Predatory polycht	Benthic bact	Benthic bact	Benthic bact

	Omnivorous crabs	Benthic algae	Meiofauna	Meiofauna
	Benthic algae	Microfauna	Benthic algae	Benthic algae
	Mesoinverts	Mesoinverts	Periphyton	Living Sediments
Graminoids	Other Macroinverts	Other Macroinverts	Floating Veg.	Periphyton
	Mink	Mink	Macrophytes	Floating Veg.
	Terrst. I	Terrst. I	Living SED	Living SED
Cypress	Snakes	Aquatic I	Cypress L	Periphyton
	Fish PC	Fish PC	Periphyton	Fish HO
	Insects	Cormorants	Diatoms	Amphipods
Lake Oneida	Leeches	Burbot	Blue-green Algae	Diatoms
	Walleye Age 0	Northern Pike	Epiphytes	Daphnia pulicaria
	Walleye Age-0	Longnose Gar	Diatoms	Diatoms
Bay of Quinte	Insects	Northern Pike	Blue-green Algae	Oligochaetes
	Yellow Perch Age 1+	Walleye Age-0	Eubosmina coregoni	Blue-green Algae
	SNKS	OTH. PP	BACT.SED.	BACT.SED.
Mangroves	TURT	INSCT	LEAF	OTH. PP
	COCO	BACT.SED.	OTH. PP	LEAF
	Predatory Shrimp	Raptors	Water Flagellates	Water Flagellates
Florida Bay	Pink Shrimp	Crocodiles	Thalassia	Benthic Flagellates
	Herbivorous Shrimp	Benthic Phytoplankton	Benthic Flagellates	Meiofauna

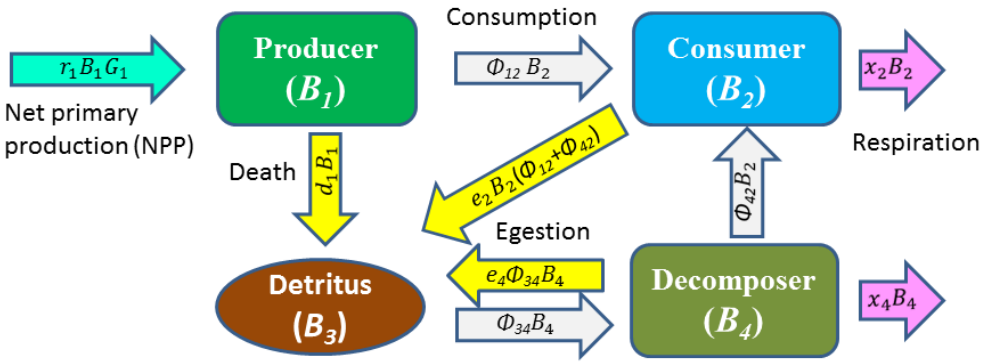

Figure S1. Scheme of dynamical model construction based on carbon flux. The food web is simplified into four compartments for clear demonstration: producers, consumers, decomposers, and detritus. The imports and exports via animal migration and water flows are considered to be in balance and not to influence the food web dynamics.

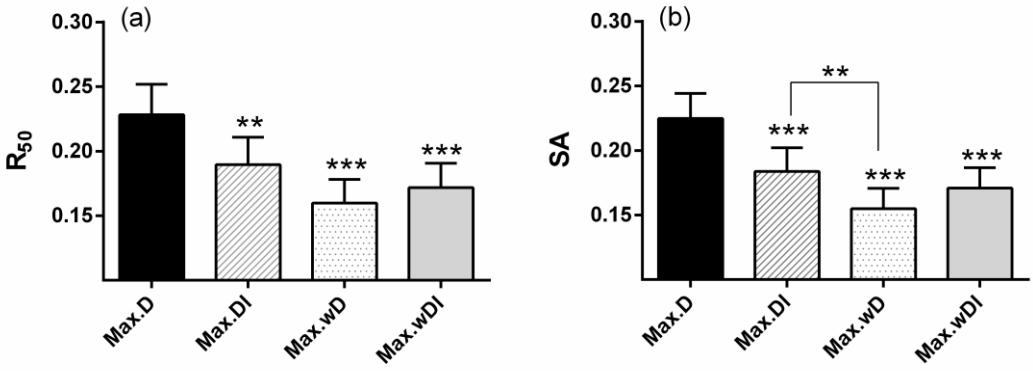

Figure S2. Stability, represented by (a) robustness, R_{50}, and (b) survival area, *SA*, to species loss in four deletion sequences (mean ± SEM) with a linear functional response. The stars directly above the error bars denote significant differences in stability between the focal deletion orders and the control order (Max.D), detected using LME and Tukey post hoc test at 0.05 level of significance. Significant differences in the stability of deletion orders Max.DI, Max.wD, and Max.wDI are indicated by stars on lines connecting the compared indices: ***$p < 0.001$; **$p < 0.01$; * $p < 0.05$; and NS, not significant.

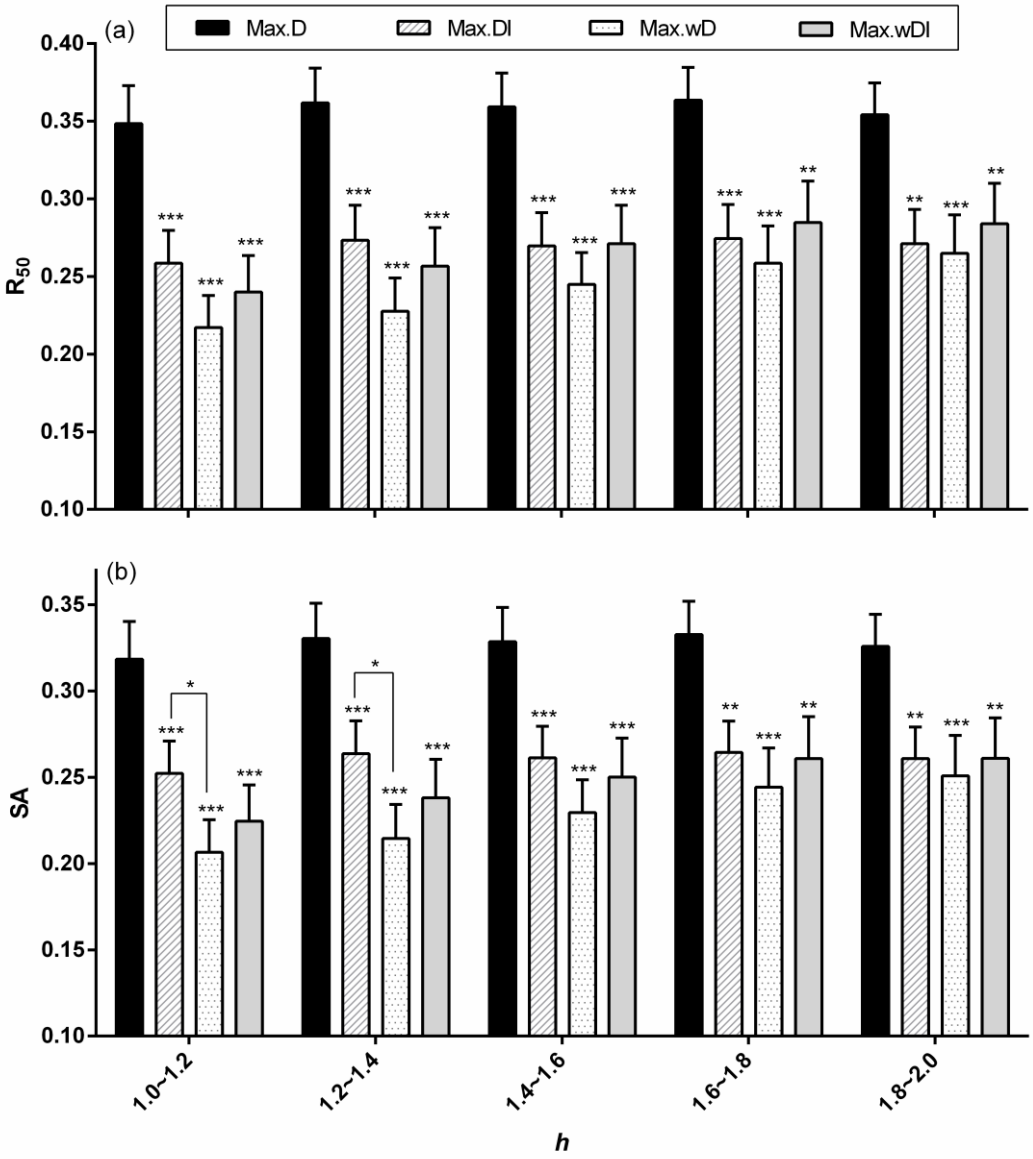

Figure S3. Stability, represented by (a) robustness, R_{50}, and (b) survival area, *SA*, to species loss in four deletion sequences (mean ± SEM) in five groups of hill exponent, *h*, with a nonlinear functional response. The stars directly above the error bars denote significant differences in stability between the focal deletion orders and the control order (Max.D), detected using LME and Tukey post hoc test at 0.05 level of significance. Significant differences in the stability of deletion orders Max.DI, Max.wD, and Max.wDI are indicated by stars on lines connecting the compared indices: ***$p < 0.001$; **$p < 0.01$; and * $p < 0.05$.

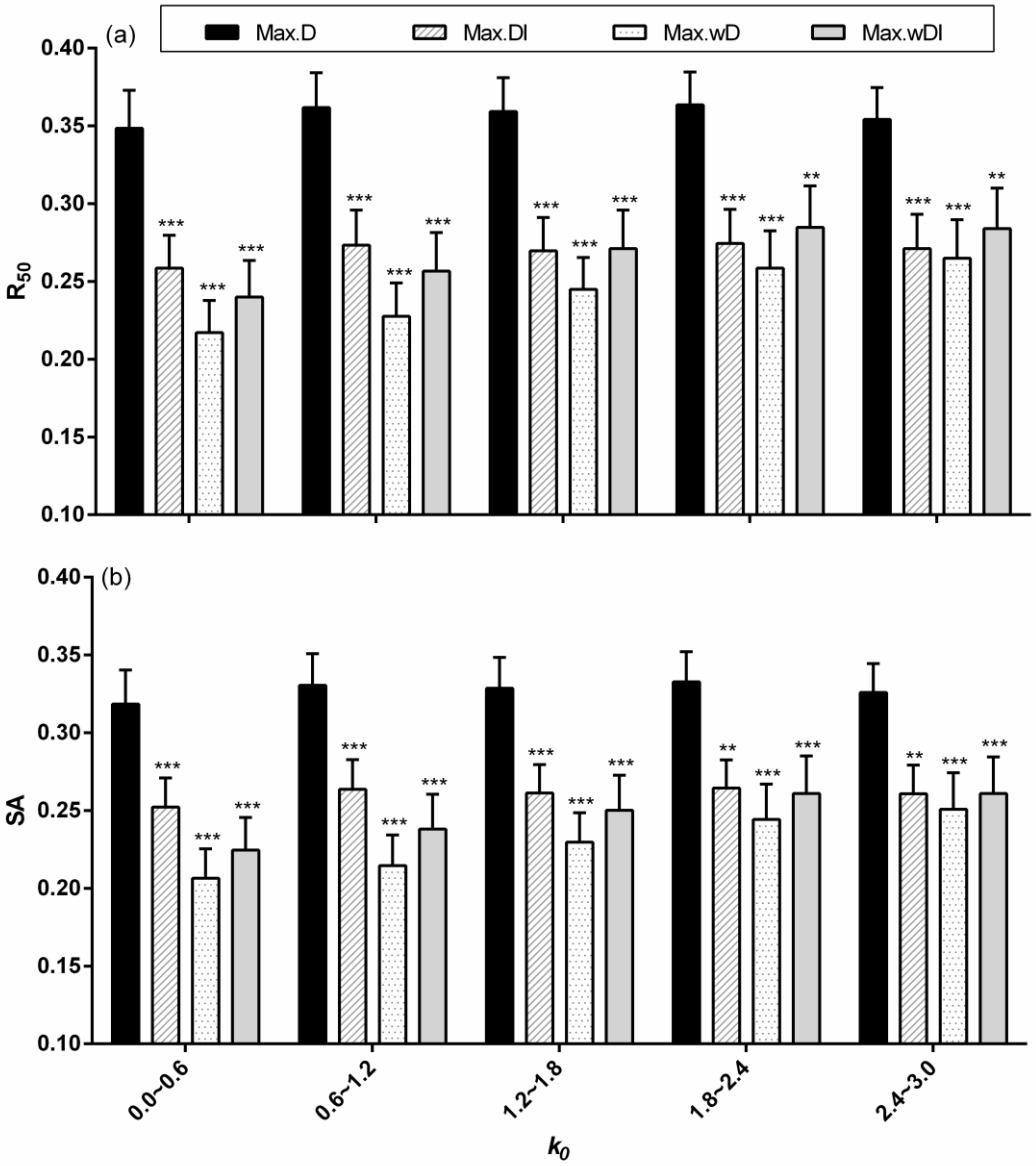

Figure S4. Stability, represented by (a) robustness, R_{50}, and (b) survival area, *SA*, to species loss in four deletion sequences (mean ± SEM) in five groups of carrying capacity coefficient, k_0, with a nonlinear functional response. The stars denote significant differences in stability between the focal deletion orders and the control order (Max.D), detected using LME and Tukey post hoc test at 0.05 level of significance: ***$p < 0.001$; **$p < 0.01$; * $p < 0.05$; and NS, not significant.

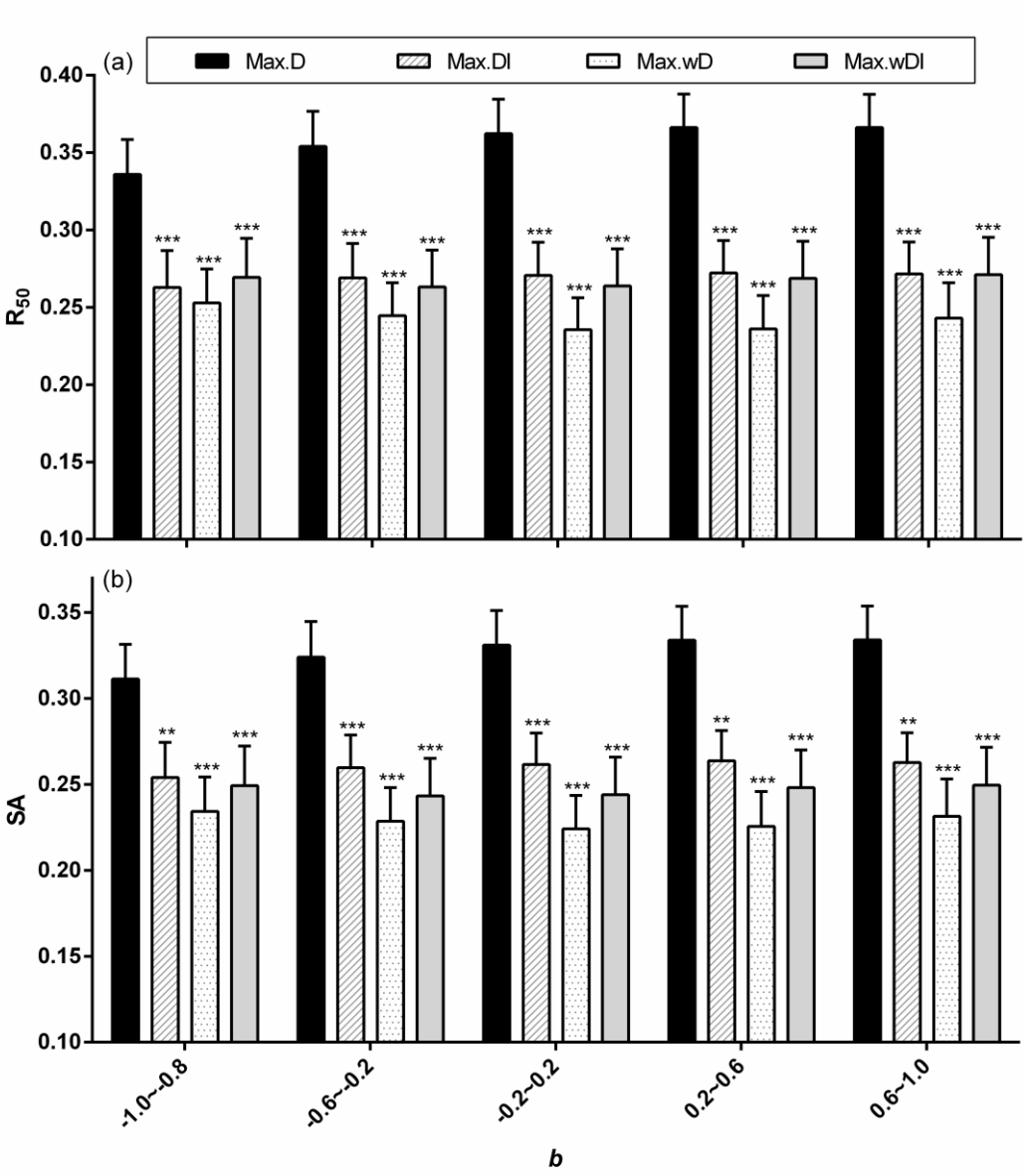

Figure S5. Stability, represented by (a) robustness, R_{50}, and (b) survival area, *SA*, to species loss in four deletion sequences (mean ± SEM) in five groups of half-saturation coefficient, *b*, with a nonlinear functional response. The stars denote significant differences in stability between the focal deletion orders and the control order (Max.D), detected using LME and Tukey post hoc test at 0.05 level of significance: ***$p < 0.001$; **$p < 0.01$; * $p < 0.05$; and NS, not significant.

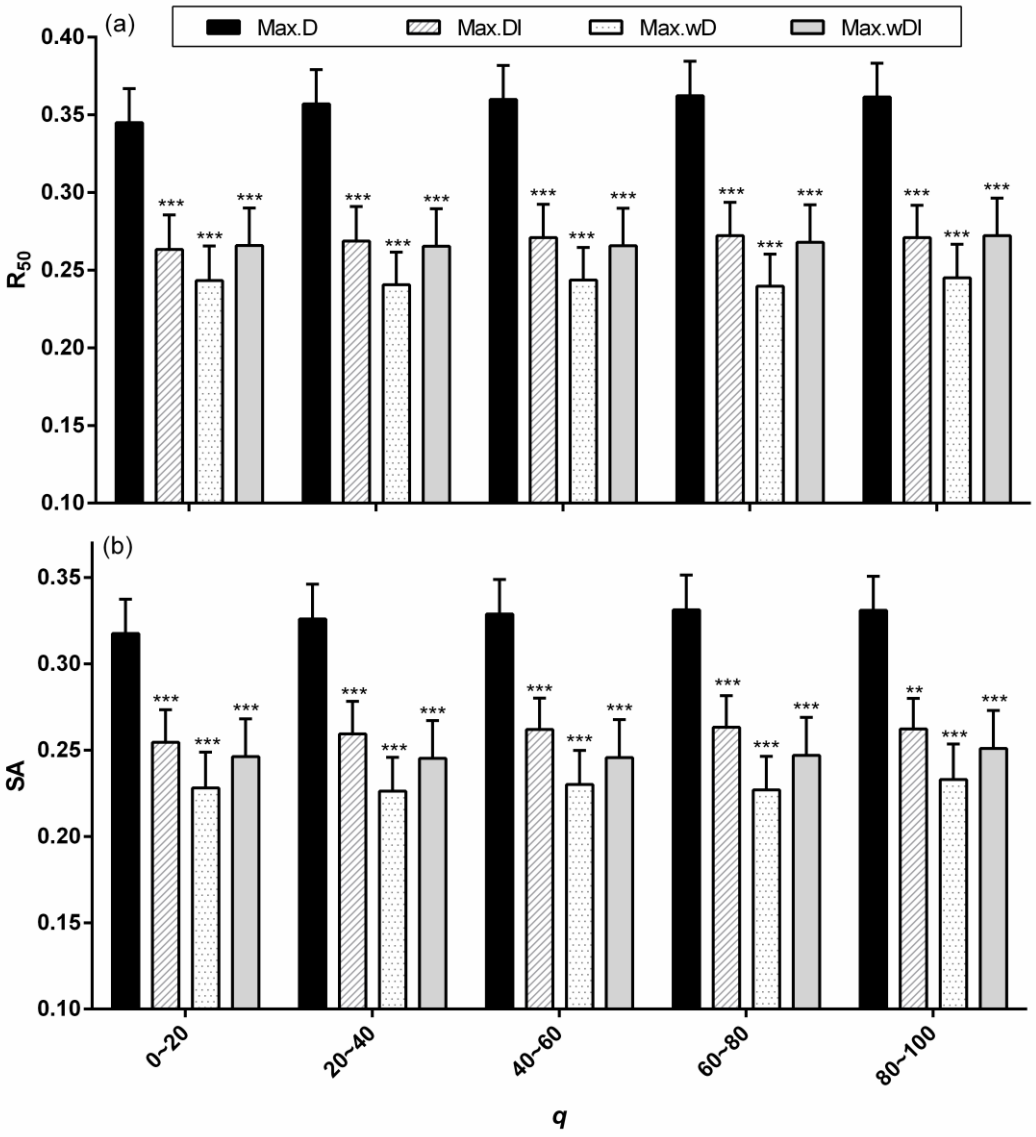

Figure S6. Stability, represented by (a) robustness, R_{50}, and (b) survival area, *SA*, to species loss in four deletion sequences (mean ± SEM) in five groups of predator interference coefficient, *q*, with a nonlinear functional response. The stars denote significant differences in stability between the focal deletion orders and the control order (Max.D), detected using LME and Tukey post hoc test at 0.05 level of significance: ***$p < 0.001$; **$p < 0.01$; * $p < 0.05$; and NS, not significant.

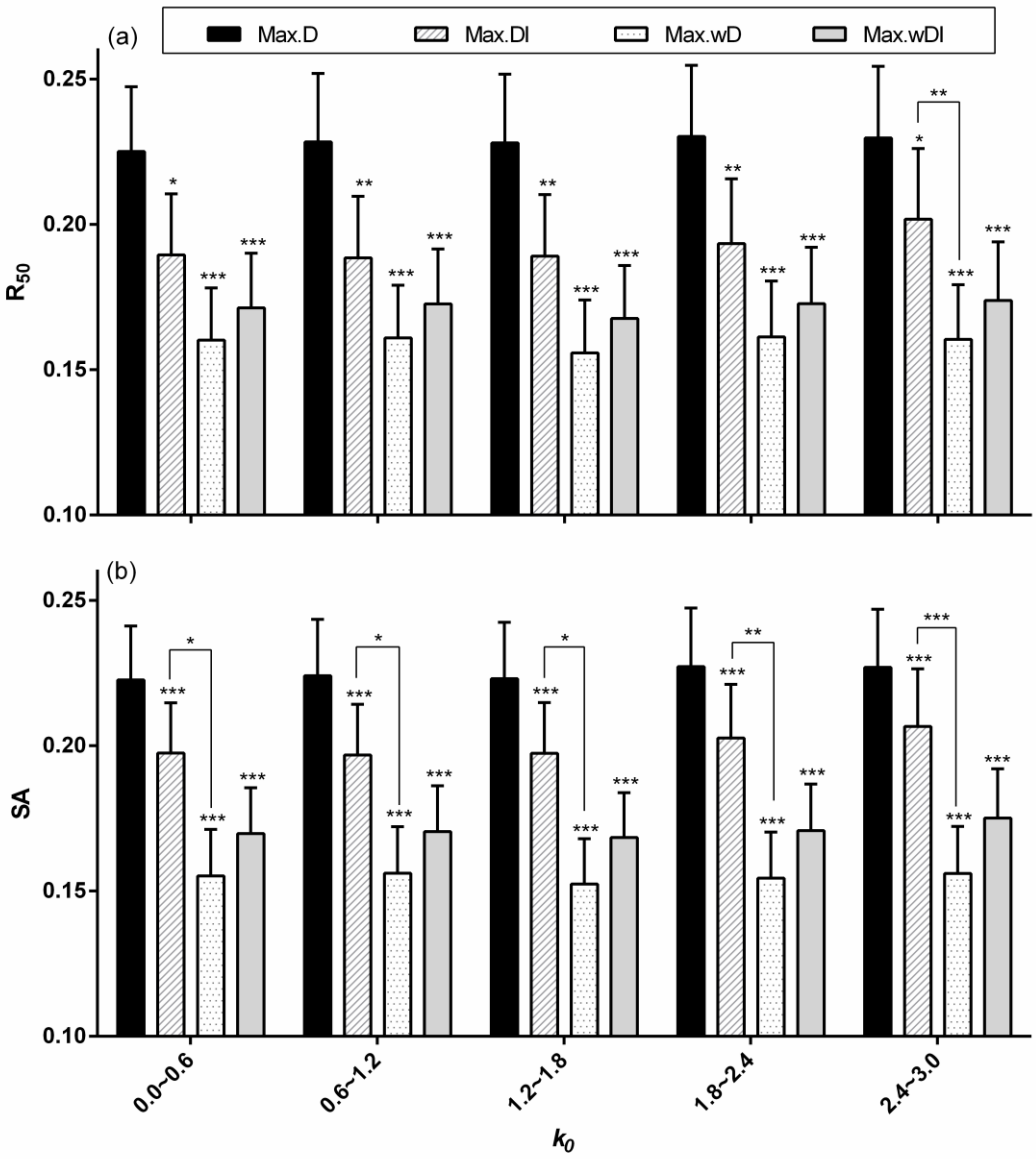

Figure S7. Stability, represented by (a) robustness, R_{50}, and (b) survival area, *SA*, to species loss in four deletion sequences (mean ± SEM) in five groups of carrying capacity coefficient, k_0, with a linear functional response. The stars denote significant differences in stability between the focal deletion orders and the control order (Max.D), detected using LME and Tukey post hoc test at 0.05 level of significance: ***$p < 0.001$; **$p < 0.01$; * $p < 0.05$; and NS, not significant.

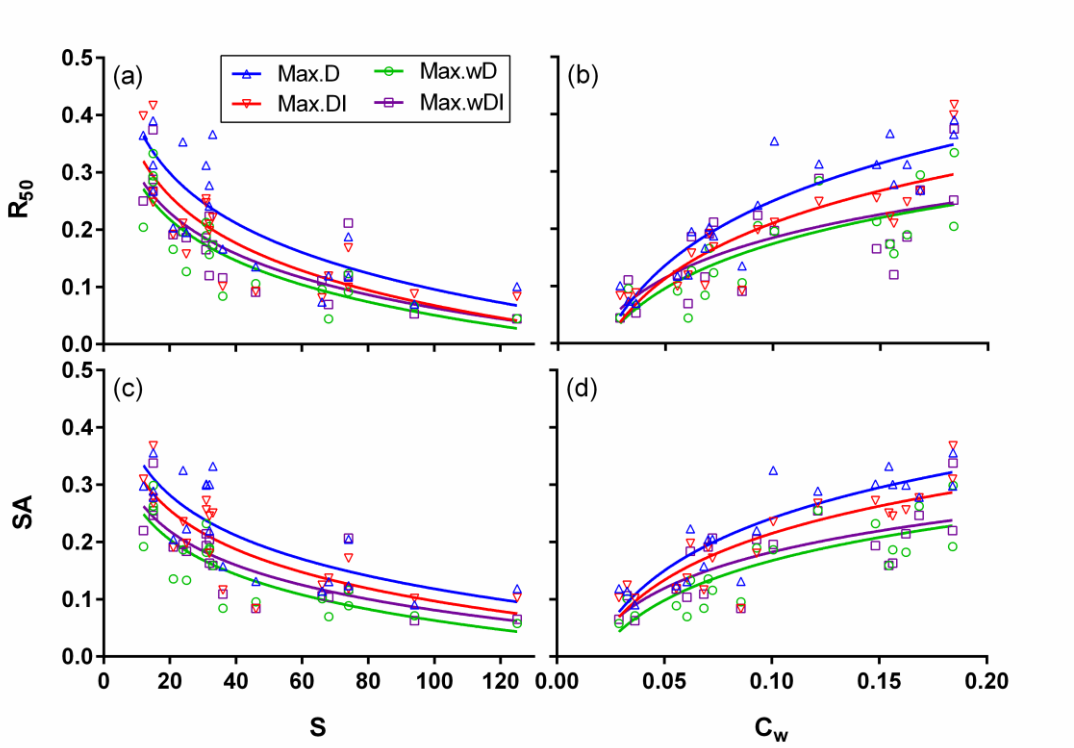

Figure S8. Stability in linear functional response simulations indicated by robustness, R_{50} (top panels), and survival area, *SA* (bottom panels), as a function of the taxon richness *S* (left panels) and weighted connectance, C_w (right panels) of each web. Logarithmic fits to the four data sets are shown, with different colours and markers indicating different deletion orders. The maximum possible *y*-value is 0.50.

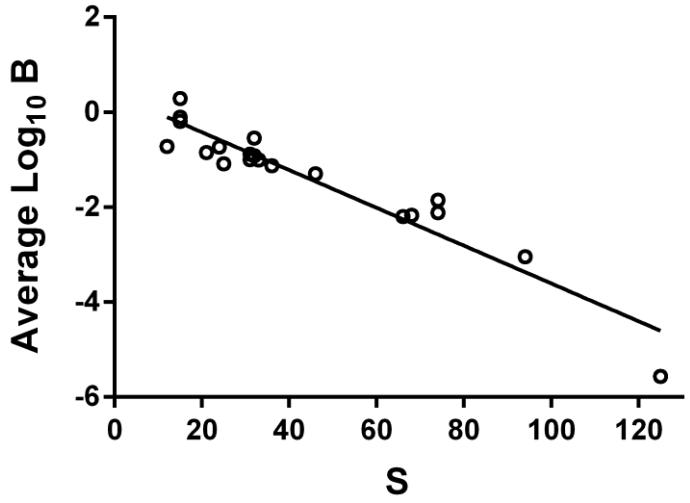

Figure S9. Linear regression of average logarithmic biomass and taxon richness of 20 food webs. The equation for the fit is Y = -0.040X + 0.377 ($F_{1,18}$ = 165.8, P < 0.001, r^2 = 0.90).

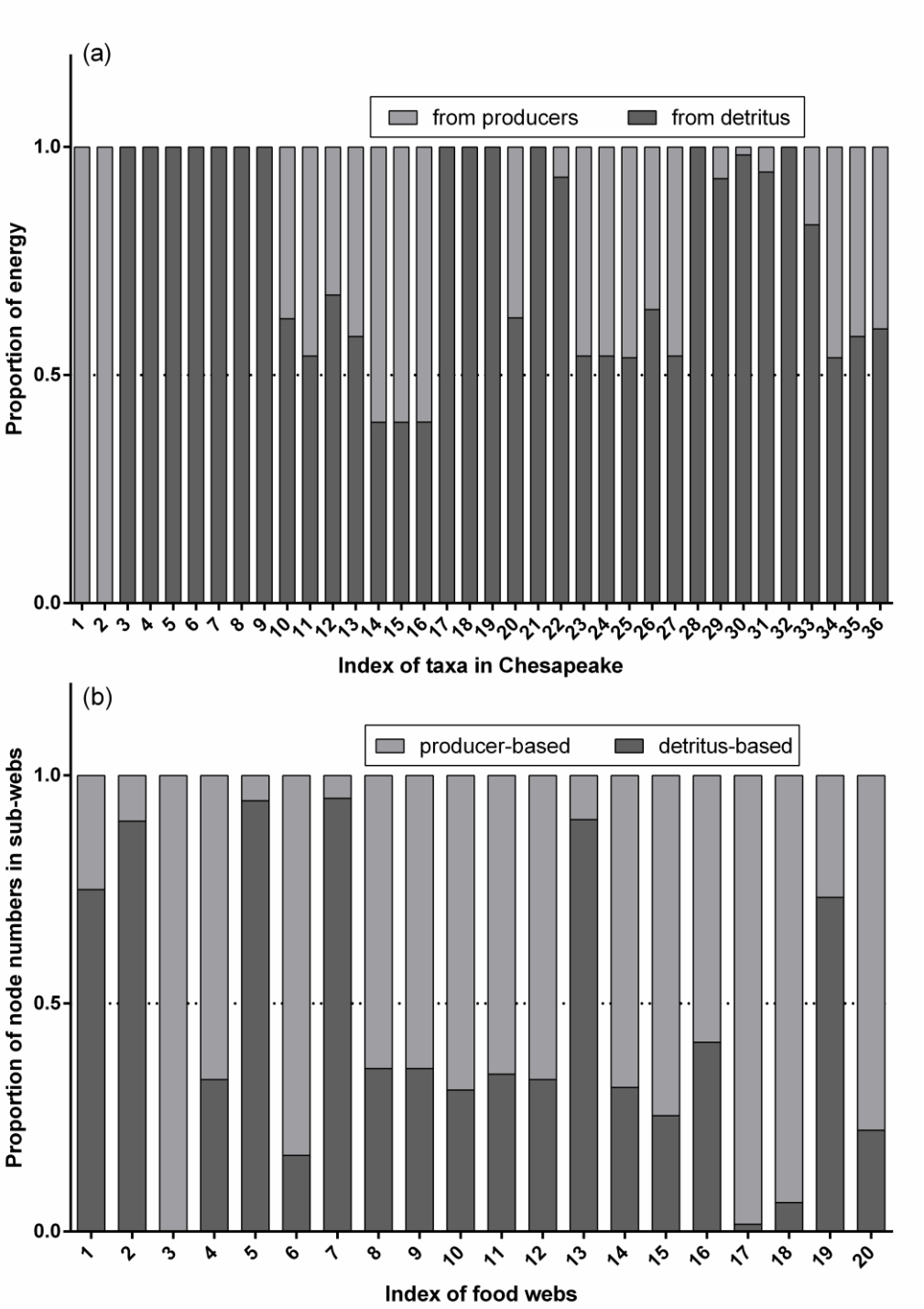

Figure S10. Comparison of energy channels from producers and detritus. (a) Proportion of energy derived from producers (grey) and detritus (dark) for each taxon in Chesapeake ecosystem. (b) Proportion of node numbers in producer-based (grey) sub-web and detritus-based (dark) sub-web for each ecosystem.

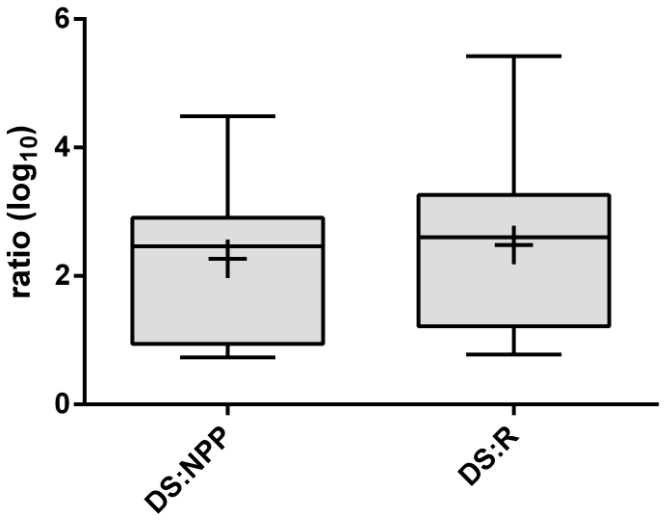

Figure S11. The ratios of detritus storage (DS) to daily net primary production (NPP) and daily respiration of the detritus-based food web (R).

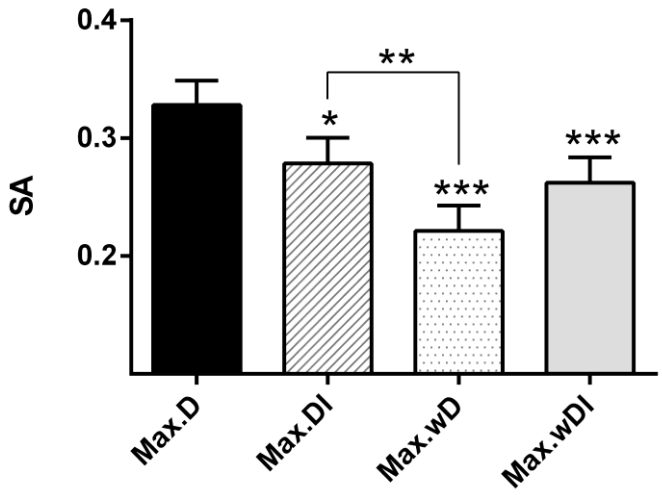

Figure S12. Stability, represented by survival area (*SA*), to species loss in four deletion sequences (mean ± SEM), when the criterion to end the simulation once all producers were extinct was applied. The stars directly above the error bars denote significant differences in stability between the focal deletion orders and the control order (Max.D), detected using LME and Tukey post hoc test at 0.05 level of significance. Significant differences in the *SA* of deletion orders Max.DI, Max.wD, and Max.wDI are indicated by stars on lines connecting the compared indices: ***$p < 0.001$; **$p < 0.01$; and * $p < 0.05$.

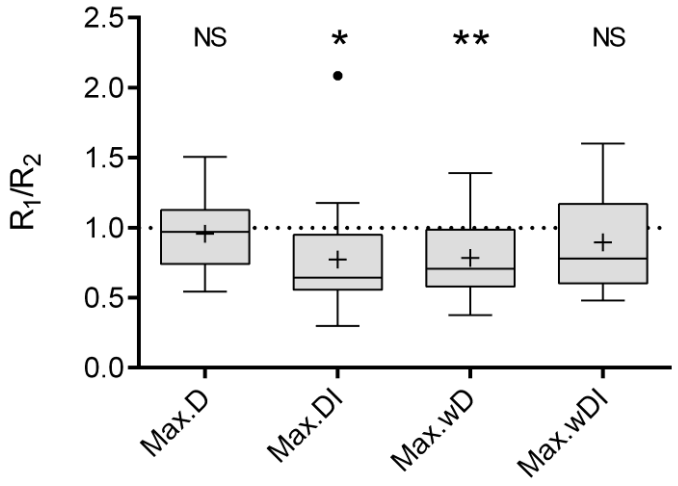

Figure S13. The ratio of the fractions of taxa that have to be removed to cause a food web to lose 0-50% (R_1) and 50-100% (R_2) of its living taxa for the four deletion sequences. Significant difference of R_1/R_2 from 1 was detected using t-test: ***p < 0.001; **p < 0.01; and * p < 0.05.

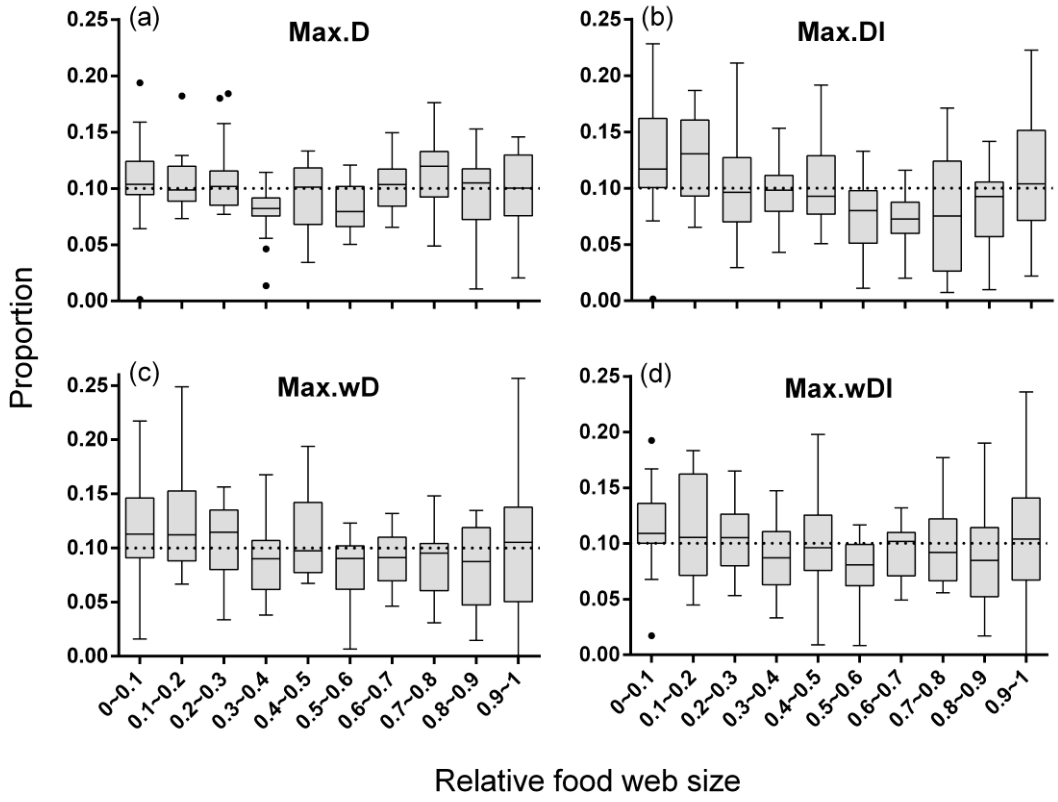

Figure S14. The proportion of relative food web sizes (the ratio of the size after deletion to the starting size) in ten size classes for the four deletion sequences.

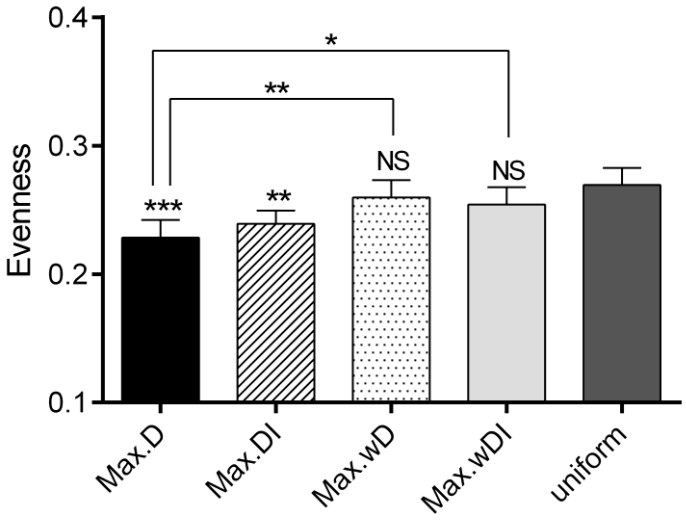

Figure S15. Pielou's evenness of the distribution of relative food web sizes in ten size classes for the four deletion sequences and uniform distribution. The stars directly above the error bars denote significant differences in evenness between the focal deletion orders and the control group (uniform), detected using LME and Tukey post hoc test at 0.05 level of significance. Significant differences in the evenness of the four deletion orders are indicated by stars on lines connecting the compared indices: ***$p < 0.001$; **$p < 0.01$; * $p < 0.05$; and NS, not significant.

Supplementary References:

Banašek-Richter C., Bersier L., Cattin M., Baltensperger R., Gabriel J., Merz Y., Ulanowicz R.E., Tavares A.F., Williams D.D. & Ruiter P.C. (2009). Complexity in quantitative food webs. *Ecology*, 90, 1470-1477.

Butler J.L., Gotelli N.J. & Ellison A.M. (2008). Linking the brown and green: nutrient transformation and fate in the Sarracenia microecosystem. *Ecology*, 89, 898-904.

Rooney N., McCann K.S. & Moore J.C. (2008). A landscape theory for food web architecture. *Ecol. Lett.*, 11, 867-881.